Evaluation of Monkman-Grant Parameters for Type 316LN and Modified 9Cr-Mo Stainless Steels

Woo Gon Kim*, Sung Ho Kim, Woo Seog Ryu

Department of Nuclear Material Technology Development, Korea Atomic Energy Research Institute, Daejon 305-600, Korea

The Monkman-Grant (M-G) and its modified parameters were evaluated for type 316LN and modified 9Cr-Mo stainless steels prepared with minor element variations. Several sets of creep data for the two alloy systems were obtained by constant-load creep tests in 550~650 ℃ temperature range. The M-G parameters, m, m', C, and C' were proposed and discussed for the two alloy systems. The m value of the M-G relation was 0.90 in type 316LN steel and 0.84 in modified 9Cr-Mo steel. The m' value of the modified relation was 0.94 in type 316LN steel and 0.89 in 9Cr-Mo steel. Although creep fracture modes and creep properties between type 316LN and modified 9Cr-Mo steels showed a basic difference, the M-G and its modified relations demonstrated linearity quite well. The m' of modified relation almost overlapped regardless of the creep testing conditions and chemical variations in the two alloy systems, and the parameter m' was closer to unity than that of the M-G relation.

Key Words : Monkman-Grant (M-G) Parameter, Creep, Type 316 LN Stainless Steel, 9Cr-Mo Stainless Steel, Steady-State Creep Rate, Rupture Time

1. Introduction

Type 316 austenitic stainless steels are candidate materials for structural components in a liquid metal reactor (LMR) because of their good high-temperature mechanical properties. Especially, the designated 'LN' grade containing low carbon (<0.03C wt.%) and an appropriate amount of nitrogen (0.1N wt.%) is superior in creep resistance to the 'L' grade of low carbon (Ryu, et al., 1998 ; Oh and Hong, 2000; Nakazawa, et al., 1988 ; Manfred and Vitale, 1984 ; Fujiwara, et al., 1986). Also, 9Cr-Mo martensitic stainless steels are prospective materials for nuclear fuel cladding tubes, and steam generator tubes in LMR due to their good thermal-fatigue strength and oxidation resistance (Berns and Krafft, 1990 ; Kim and Ryu, 2000). Since these structural components of nuclear power plants are operated at high temperatures, one of the most critical factors in determining the integrity of their components is creep behavior. Due to thermal activation, the materials can slowly and continuously deteriorate under constant load or stress even below the yield stress levels, and eventually fail (Viswanathan, 1989).

The design of high-temperature creeping materials has to be based on reliable long-term test data beyond its design life. However, these long-term data are not available for many materials, because it is time-consuming and expensive to obtain the appropriate data. Therefore, design of creep components is carried out by extrapolation of short-term creep data to approximate the long-term behavior. One of the most common methods is known as the Monkman and Grant (hereafter M-G) relation (Cadek, 1988 ; Nabarro and Villers, 1995). A log-log plot of rupture time, t_r, versus steady-state creep rate (or minimum creep rate), $\dot{\varepsilon}_s$, shows empirically a straight line

* Corresponding Author,
E-mail : wgkim@kaeri.re.kr
TEL : +82-42-868-2493; **FAX** : +82-42-868-8346
Department of Reactor Core Materials, Korea Atomic Energy Research Institute, P.O. Box 105 Yusong, Daejon, 305-600, Korea. (Manuscript **Received** January 26, 2002; **Revised** August 13, 2002)

as follows:

$$\log t_r + m \log \dot{\varepsilon}_s = C \quad (1)$$

where m and C are the M-G parameters. If the parameters, m and C are obtained, the rupture time can be assessed on the basis of steady-state creep rate, $\dot{\varepsilon}_s$. The C parameter of Eq. (1) depends on the temperature and the material.

The modified relation has been proposed using the total strain at rupture, ε_r and the stress and temperature dependence can be reduced as follows. (Dobes and Milicka, 1976);

$$\log \left(\frac{t_r}{\varepsilon_r}\right) + m' \log \dot{\varepsilon}_s = C' \quad (2)$$

The exponent m' is close to unity, and C' parameter is independent of the temperature. ε_r is closely related to creep deformation processes which lead to the formation of cracks and cavities. Therefore, ε_r is considered as another important parameter. The validity of this modified M-G model was in excellent agreement with creep rupture experiments Performed using several materials: 2.25 Cr-1 Mo steels, martensitic zirconium alloys, 25Cr-20Ni austenitic stainless steel, etc (Cadek, 1988; Nabarro and Villers, 1995; Dobes and Milicka, 1976). However, a practical evaluation of the relations on type 316LN and 9Cr-Mo stainless steels for the LMR application has not been established, and the creep data or parameters for the two alloys are insufficient.

The purpose of this work was to evaluate the M-G and its modified relations for type 316LN and 9Cr-Mo stainless steels, and to propose their parameters. Several sets of creep data were measured for the two alloy systems and the fracture micrographs were observed to define the differences.

2. Experimental Procedures

Laboratory ingots of type 316LN and 9Cr-Mo alloys were prepared by the vacuum induction melting (VIM) process. Their chemical compositions are given in Table 1. Type 316LN alloy contains around 0.1 wt.% nitrogen and 9Cr-Mo alloy has minor elements such as vanadium (V), niobium (Nb) and tungsten (W). The ingots were held for 2 hr at 1150 ℃ in an argon atmosphere and reduced to 15 mm thickness by a hot rolling process. Type 316LN alloy was solution annealed at 1100 ℃ for 1 hr and water quenched. The 9Cr-Mo alloy was heat treated by normalizing and tempering. Normalizing was performed at 1050 ℃ for 1 hr and air cooled, and then tempering was performed at 750 ℃ for 2 hr and air cooled. Creep specimens were taken along the rolling direction and machined in cylindrical form with a 30 mm gauge length and 6 mm diameter. The gauge sections of the specimens were polished using 1000 grit sand paper along the specimen axis.

Creep tests were conducted using constant-load machines with a 20/1-lever arm ratio. The test temperature was maintained to be constant within ±2 ℃ during the test period. Before starting the test, all specimens were held at the test temperature for 1 hr. All creep test procedures were followed according to the ASTM standard (ASTM E139, 1983). Creep strain was measured using either an extensometer gauge or a precise dial indicator. The steady-state creep rate (SSCR) was calculated by Eq. (3), using creep strain (dl) with time variation (dt) in the secondary creep region,

$$\dot{\varepsilon}_s = \frac{d[(l_2 - l_1)/l_o]}{dt} = \frac{1}{l_o}\frac{dl}{dt} \quad (3)$$

Table 1 Chemical compositions of type 316LN and modified 9Cr-Mo stainless steels(wt.%)

	C	Si	Mn	P	S	Cr	Ni	Mo	N	B	V	Nb	W
316LN	0.021	0.70	0.97	0.002~0.021	0.006	17.30	12.34	2.36	0.10	0~0.0050	—	—	
9Cr-Mo	0.15	0.08	0.48	0.002	0.004	9.94	0.49	1.27	0.02	—	0.203~0.310	0.195	0~0.450

where l_o is the initial gauge length of the specimen.

After testing, each specimen was examined for microstructures; fracture surfaces, cavities, and precipitates using scanning electron microscopy (SEM). A thin disk of the creped specimen was taken from the center part of the gauge section along the stress axis. For the SEM analysis, etching of type 316LN steel took place in the mixture of 10% hydrochloric acid +15% acetic acid +10% nitric acid +65% distilled water, and etching of the 9Cr-Mo steel in the mixture of 2% hydrofluoric acid +2% nitric acid +96% distilled water.

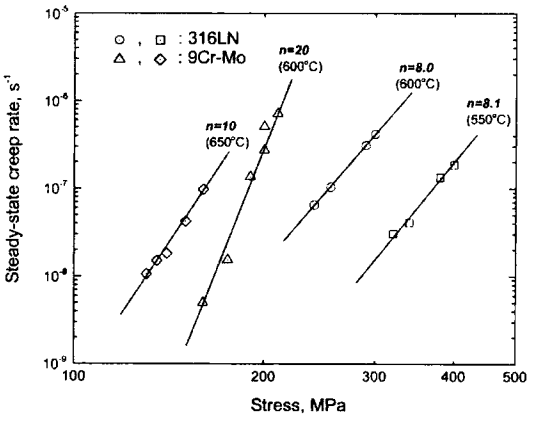

Fig. 1 Typical plot of steady-state creep rate with stress and temperature for type 316LN and modified 9Cr-Mo stainless steels

3. Results and Discussion

3.1 Creep strain curves

The steady-state creep rate and the rupture time are considered as important features in creep properties. Therefore, these two factors are generally described to be a function of temperature and stress; $\dot{\varepsilon}_s = f(\sigma, T)$ and $t_r = g(\sigma, T)$. The dependence of the creep rate on applied stress can be written as a power law (or Norton's law) of Eq. (4).

$$\dot{\varepsilon}_s = A\sigma^n \tag{4}$$

It can be characterized by the sensitivity parameter of the steady-state creep rate to applied stress, n':

$$n' = \left(\frac{\partial \ln \dot{\varepsilon}_s}{\partial \ln \sigma}\right)_T \tag{5}$$

where A is a constant at a given temperature and n is the stress exponent. Under temperature and stress conditions used in this work, a creep deformation map for the two alloy systems corresponds to dislocation creep regime which yields the power law of stress dependence (Kim, et al., 2000; Penny and Marriott, 1995). Thus, the exponent n in this work can be written as $n = n'$ because of dislocation creep mechanism. The value of n can be determined by the slope of log $\dot{\varepsilon}_s$-log σ plot.

Figure 1 shows typical results of the steady-state creep rate with various stresses in 550~650 ℃ temperatnre range of type 316LN and 9Cr-Mo stainless steels. The n value of type 316LN stainless steel was not changed with temperatures as it was 8.0 at 600 ℃ and 8.1 at 550 ℃. It was similar to 7.9 that Frost and Ashby have reported at 650 ℃ for commercial type 316 stainless steel (Riedel, 1987). However, the n value for 9Cr-Mo martensitic stainless steel was greatly changed with temperatures as it was 20 at 600℃ and 10 at 650 ℃. The 9Cr-Mo steel resulted in greater n value than type 316LN steel. This means that 9Cr-Mo steel showed significant temperature dependency due to high or low thermal stability during creep. As for the valas of exponent n, Cadek (1988) and Evans et al. (1985) had reported it to be between 4 to 5 typically for dislocation creep in pure metal, and as great as 10 in precipitation and dispersion strengthened metallic materials, and in the range from 3 to 13 in commercial and laboratory melted austenitic stainless steels. From these results, the n value of 9Cr-Mo steel was higher than that of type 316LN steel, and its value showed a high temperature dependency.

Figure 2 shows the typical creep-rupture curves of type 316LN and 9Cr-Mo stainless steels, where creep strain is the difference between the creep strain, ε_c, and the instantaneous strain, ε_0. The two steels showed large differences in the creep deformation curve. Most of the rupture time of 9Cr-Mo steel was occupied with the secondary creep stage, and the creep strain was much lower

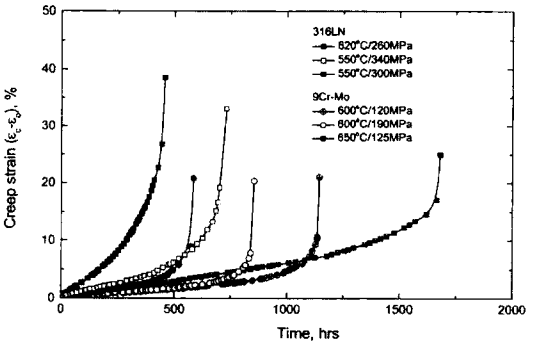

Fig. 2 Typical creep curves for type 316LN and modified 9Cr-Mo stainless steels

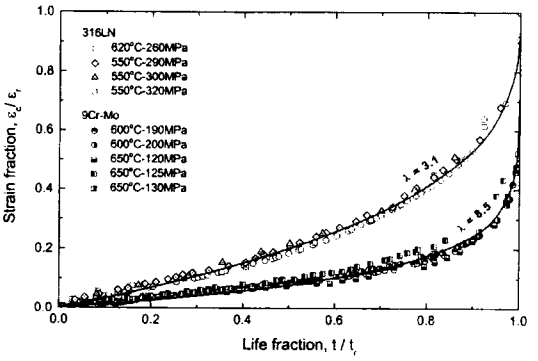

Fig. 3 Comparison of strain fraction vs. life fraction for type 316LN and modified 9Cr-Mo stainless steels

than that of type 316LN steel. In spite of that, 9Cr-Mo steel was shorter in rupture time than type 316LN steel. This means that 9Cr-Mo steel was inferior in creep ductility to type 316LN steel, and most of the creep strain was suddenly increased near the rupture time. It is believed that 9Cr-Mo steel experienced ductile fracture leading to a localized neck near the fracture. Therefore, the two alloy systems were basically different in fracture types. To clarify this fact for the two alloy systems, Kim et al. (2001) have reported in a previous study on the creep master curves between the strain fraction ($\varepsilon_c/\varepsilon_r$) and life fraction ($t/t_r$) using the Kachanov-Rabotnov (K-R) creep damage model, as shown in Fig. 3. Figure 3 shows the comparison of the creep curves on strain fraction ($\varepsilon_c/\varepsilon_r$) versus life fraction ($t/t_r$) for type 316LN and 9Cr-Mo steels. The symbol marks indicate the measured points and the solid lines indicate the curves calculated by the K-R model, where ε_r is the rupture elongation, t_r is the rupture time, and ε_c is the current creep strain. All of the measured data showed material dependence regardless of testing conditions, applied stress or temperatures. For the relation of creep strain and time fraction, using the K-R creep model defined as Eq. (6) (Kim, et al., 2001 ; Penny and Marriott, 1995),

$$\frac{\varepsilon_c}{\varepsilon_r}=\left[1-\left(1-\frac{t}{t_r}\right)^{1/\lambda}\right]=\varepsilon^*\lambda\left[1-\left(1-\frac{t}{t_r}\right)\right]^{1/\lambda} \quad (6)$$

the creep tolerance parameter, λ becomes a sensible constant which determines the shape of the creep curves. The value of λ in this work was determined by fitting the experimental data as 3.1 for type 316LN and 8.5 for 9Cr-Mo. The creep curves and creep rupture strain were different.

3.2 The M-G parameters

Figure 4 shows the slope m of the M-G relation obtained from rupture time versus steady-state creep rate for type 316LN and 9Cr-Mo steels. The individual points in the plots represent all experimental data with testing stresses, temperatures, and minor element variations. Each plot of type 316LN and 9Cr-Mo steels showed

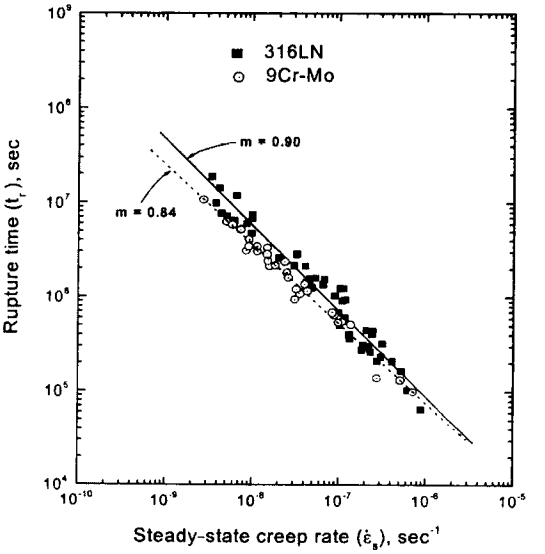

Fig. 4 Comparison of rupture time vs. steady-state creep rate for type 316LN and modified 9Cr-Mo stainless steels

Table 2 Summary of test values and equation constants

	Experimental values		M-G relation (Eq. 1)		Modified relation (Eq. 2)	
	Temp. range, ℃	No. of points	m	C	m^*	C^*
316LN	550~600	49 points	0.90	−0.5073	0.94	−0.2517
9Cr-Mo	600~650	32 points	0.84	−0.1697	0.89	0.1244

good linearity as exprtssed by Eq. (1). The value of m was found to be slightly different for the two steels: m=0.90 in type 316LN steel and m=0.84 in 9Cr-Mo steel. The value of m has been reported to be in the range of about 0.8 to about 0.95, and the parameter C depends on the temperature (Cadek, 1988). Kim et al. (2000) have reported m=1.0~1.3 range in close inspection with variation of phosphorous (P) element for type 316LN steel. The slight difference in the m value in type 316LN was because Kim's previous study was investigated for only phosphorous effect on creep properties. Type 316LN steel is superior in creep life to 9Cr-Mo steel. Although the two steels were highly different in the n or λ parameters due to rupture time and creep ductility, the m values of the M-G relation did not vary greatly in the reported range. The computed values of the m and C parameters are listed in Table 2.

In addition, the existence of such a relationship as Eq. (1) between the rupture time and the steady-state creep rate leads to some interesting speculations concerning some aspects of the creep process. If the slope m is unity, the M-G relation can be rewritten in the following form,

$$t_r \cdot \dot{\varepsilon}_s = C \tag{7}$$

From Table 2, slope m is appreciably 1. Therefore, Eq. (7) is approximately correct for the two alloy systems and it can be simply utilized to estimate the long-time data from the short-time data.

3.3 Modified M-G parameters

Figure 5 shows the modified M-G relation using t_r/ε_r for type 316LN and 9Cr-Mo steels. The value of slope m' was 0.94 in type 316LN steel and 0.89 in 9Cr-Mo steel. For a given creep rate, it can be seen that type 316LN austenitic

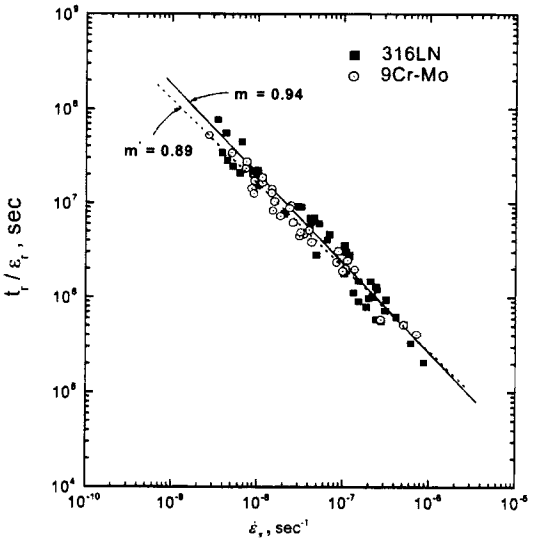

Fig. 5 The log-log plot between t_r/ε_r and $\dot{\varepsilon}_s$ for type 316LN and modified 9Cr-Mo stainless steels

steel takes a longer time to rupture than 9Cr-Mo steels. Howerer the modified M-G curves were nearly overlapped regardless of the chemical variations and testing conditions for the two steels. The parameter m' of the modified relation clearly demonstrates the superiority over parameter m of the original M-G relation, and also parameter m' is closer to unity than m. It means that the creep rupture elongation has a close relationship with the rupture time.

Figure 6 shows all the data points of the rupture elongation and the rupture time for type 316LN and 9Cr-Mo stainless steels. The rupture elongation decreased inversely with increasing rupture time. The rupture elongation of type 316LN steel was higher than that of 9Cr-Mo steel. It means that the rupture elongation increases with decreasing steady-state creep rate. Scatter in the data of type 316LN steel is wider than that of 9Cr-Mo steel. This, for type 316LN

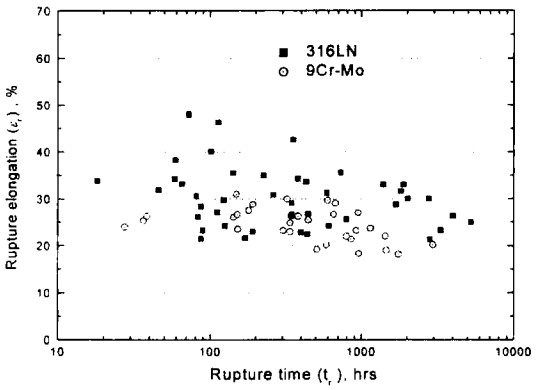

Fig. 6 Data points between rupture time and rupture elongation for type 316LN and modified 9Cr -Mo Stainless steels

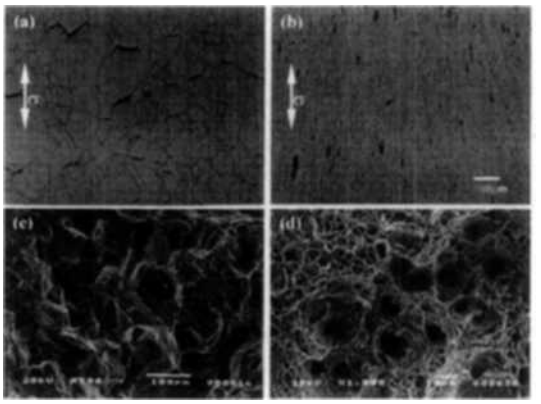

Fig. 7 Typical fracture micrographs of type 316LN (a, c) and modified 9Cr-Mo(b, d) stainless steels specimens ; 316LN steel is at 300 MPa/ 600 ℃, and 9Cr-Mo steel is at 190 MPa/ 600 ℃

stainless steel, was due to variety in the chemical variations. All the points showed the tendency of material dependence, although t_r and ε_r data were different with testing conditions or chemical variations.

From the results, it is believed that the modified relation including the rupture elongation has a close connection with deformation processes, which lead to the formation of cracks and cavities and to final rupture. Furthermore, it means that Eq. (2) indicates one process typically controlling the creep strain during the whole test at various creep stages. It is noted that the modified relation was improved in applicability compared with the M-G relation although the creep properties of type 316LN and 9Cr-Mo steels were basically different in crystal structures. To define the applicability of the M-G relation and the fracture microstructures, creep fracture micrographs for two alloy systems were investigated as described in the following section.

3.4 Creep fracture micrographs

Figure 7 shows the fracture micrographs for type 316LN and 9Cr-Mo stainless steels. The fracture modes of the two steels were greatly different as seen in Figs 7 and 8. OM micrographs (a) and (b) in Fig. 7 show creep cracks along the longitudinal direction just below the fracture surface, and (c) and (d) show the fracture surfaces. In the fracture mode, type 316LN steel showed domination of intergranular fracture and the crack path propagated along the grain boundaries. Wedge type cracks at triple junction points were also observed. The fracture of type 316LN steel was caused by the growth and incorporation of cavities. Also the cavities were distributed perpendicular to the stress axis, as shown in Fig. 7(a). On the contrary, the fracture of 9Cr-Mo steel showed transgranular fracture of ductile type caused by the softening of materials. Cavity cracks were not observed and only small size voids were observed locally at the center of the neck. They were axially deformed along the stress axis shown in Fig. 7(b). The reduction of area at its neck was higher than that of type 316LN steel and the rupture elongation was inversed. It is noted that the fracture of 9Cr-Mo steel occurred suddenly by the softening of the material at a high temperature without a symptom, and that its fracture mode was typical cup-and-cone ductile fracture with a localized necking (Kim et al., 2001).

Furthermore, the two alloy systems showed the basic difference from the morphology of the precipitates in the grain boundary. The precipitate morphologies of 316LN and 9Cr-Ni steels are shown in Fis. 8. The precipitates of type 316LN steel were distributed in blocks along the grain boundaries which become nucleation sites of cav-

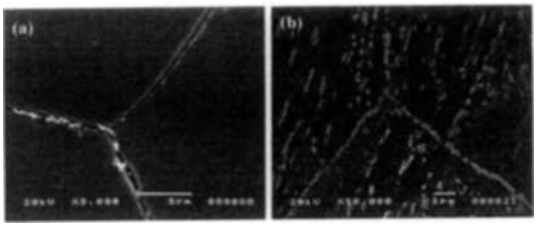

Fig. 8 Precipitate morphology in grain boundary for type 316LN(a) and 9Cr-Mo(b) specimens; 316LN steel is at 300 MPa/600 ℃ and 9Cr -Mo steel is at !90 MPa/600 ℃

ities or voids. However, the precipitates of 9Cr-Mo steel were distributed continuously along lathe-boundaries or prior-austenitic grain boundaries. At a high temperature the precipitates grow coarsely and become discontinuous. The two alloy systems were basically different in creep fracture morphologies as well as in creep properties. In spite of these differences, the M-G relation showed a reliable agreement regardless of the creep testing conditions and minor element variations. This agreement is due to the fact that the two alloy systems showed the same dislocation creep mechanism relevant to the middle homologous temperature from 0.40 T_m to 0.44 T_m.

4. Conclusions

The M-G and its modified parameters for modified type 316LN and modified 9Cr-Mo stainless steels were evaluated using the creep data obtained by constant-load creep tests in 550~650 ℃ temperature range. In spite of the basic differences in creep fracture modes and creep properties for the two alloys systems, the M-G relation demonstrated linearity regardless of the creep testing conditions and chemical variations. The value of the m parameter of the M-G relation was found to be slightly different for the two alloy systems ; m=0.90 for type 316LN steel and m= 0.84 for 9Cr-Mo steel. Also, the value of the m' parameter of the modified relation was 0.94 for type 316LN steel and 0.89 for 9Cr-Mo steel. Type 316LN austenitic stainless steel has a greater rupture time than 9Cr-Mo martensitic stainless steel. The difference in the m and m' parameters was due to different elongation values at fracture. It was identified that the modified relation was superior to the M-G relation because the m' slopes almost overlapped regardless of the creep testing conditions for the two materials.

Acknowledgment

This work is a part of the Nuclear Material Development Project, which has been financially supported by the Korean Ministry of Science and Technology.

References

ASTM standard, 1983, "Standard Practice for Conducting Creep, Creep-Rupture, and Stress -Rupture Tests of Metallic Materials," *ASTM E139*, pp. 305~314.

Berns, H. and Krafft, F., 1990, "12%Cr Steels Alloyed with Nitrogen under Pressure and The Influence of A Thermo-mechanical Treatment on Their Mechanical Properties," *Proc. of the Conf. on Rupture Ductility of Creep Resistance Steels*, Edited by Strang, A., held at York, pp. 116~124.

Cadek, J. 1988, Creep in Metallic Materials, *Material Science Monographs*, Vol. 48, Elsevier, Amsterdam-Oxford-New York-Tokyo, pp. 335~338.

Dobes, F. and Milicka, K. 1976, "The Relation Between Minimum Creep Rate and Time to Fracture," *Metal Science*, Vol. 10, pp. 382~384.

Evans, R. W. and Wilshire, B., 1985, Creep of Metals and Alloys, *The Institute of Metal*, London, pp. 9~12.

Fujiwara, M., Uchida, H., Ohta, S., Yuhara, S., Tani, S. and Sato, Y., 1986, "Development of Modified Type 316 Stainless Steel for Fast Breeder Reactor Fuel Cladding Tubes," *Radiation-Induced Change in Microstructure 13th Int., Sym. -Part I, ASTM STP 955*, pp. 127~145.

Kim, W. G., Kim, D. W. and Ryu, W. S., 2000, "Applicability of Monkman-Grant Relationships to Type 316L(N) Stainless Steel," *Transactions of the KSME, A*, Vol. 24, No. 9, pp. 2326~2333.

Kim, W. G., Kim, D. W. and Ryu, W. S., 2001,

"Creep Design of Type 316LN Stainless Steel by K-R Damage Theory," *Transactions of the KSME, A*, Vol. 25, No. 2, pp. 296~303.

Kim, W. G. and Ryu, W. S., 2000, "Application of K-R Creep Damage Constitutive Equation to Type 316LN Stainless Steel," *Proc. of Materials and Fracture Part of the KSME-00MF078*, Sungkyunkwan University, pp. 232~238.

Kim, W. G., Kim, S. H. and Ryu, W. S., 2001, "Creep Characterization of Type 316LN Stainless Steel and HT-9 Stainless Steels by the K-R Damage Model," *KSME International Journal*, Vol. 15, No. 11, pp. 1463~1471.

Manfred, E. and Vitale, E., 1984, "Creep Strength and Hot Tensile Behavior in AISI 316 Austenitic Steels," *Proc. of the 2nd International Conference on Creep and Fracture of Engineering Materials and Structures-Part II*, Edited by B. Wilshire and D. R. J. Owen, Pineridge Press, Swansea, U. K., pp. 1239~1249.

Nabarro, F. R. N. and Villers, H. L., 1995, The Physics of Creep-Creep and Creep-Resistant Alloys, *Taylor & Francis Ltd*, pp. 22~26.

Nakazawa, T., Abo, H., Tanino, M., Komatsu H., Nishida, T. and Tashimo, M., 1988, "Effect of Nitrogen and Carbon on Creep Properties of Type 316 Stainless Steels," *Proc. of High Nitrogen Steels-HNS 88*, held at Lile in France, pp. 218~223.

Oh, Y. J. and Hong, J. H., 2000, "Nitrogen Effect on Precipitation and Sensitization in Cold-Worked Type 316L(N) Stainless Steel," *Journal of Nuclear Materials*, Vol. 278, pp. 242~250.

Penny, R. K. and Marriott, 1995, D. L., Design for Creep, *Chapman & Hall*, London, pp. 139~199.

Riedel, H., 1987, Fracture at High Temperature, *Material Research and Engineering*, Edited by Ilschner, B. and Grant, N. J., Springer Verlag, pp. 389~390.

Ryu, W. S., Kim, W. G., Kim, D. W., Kuk, I. H., Jang, J., Rhee, C. K., Chung, M. G., Park, S. D. and Han, C. H., 1998, "A State of the Art Report on LMR Structure Materials," *KAERI/AR-487/98*, pp. 37~47.

Viswanathan, R., 1989, Damage Mechanisms and Life Assessment of High-Temperature Components, *ASM International*, pp. 10~18.